

ChemComm

Accepted Manuscript



This is an *Accepted Manuscript*, which has been through the Royal Society of Chemistry peer review process and has been accepted for publication.

Accepted Manuscripts are published online shortly after acceptance, before technical editing, formatting and proof reading. Using this free service, authors can make their results available to the community, in citable form, before we publish the edited article. We will replace this *Accepted Manuscript* with the edited and formatted *Advance Article* as soon as it is available.

You can find more information about *Accepted Manuscripts* in the [Information for Authors](#).

Please note that technical editing may introduce minor changes to the text and/or graphics, which may alter content. The journal's standard [Terms & Conditions](#) and the [Ethical guidelines](#) still apply. In no event shall the Royal Society of Chemistry be held responsible for any errors or omissions in this *Accepted Manuscript* or any consequences arising from the use of any information it contains.

COMMUNICATION

Efficient alkene hydrogenation over magnetically recoverable and recyclable Fe₃O₄@GO nanocatalyst using hydrazine hydrate as the hydrogen source†

Cite this: DOI: 10.1039/x0xx00000x

Received 00th January 2012,
Accepted 00th January 2012John Mondal,^a Kim Truc Nguyen,^a Avijit Jana,^a Karina Kurniawan,^a Parijat Borah,^a
Yanli Zhao^{*ac} and Asim Bhaumik^{*b}

DOI: 10.1039/x0xx00000x

www.rsc.org/

Magnetic Fe₃O₄ nanoparticles embedded on Graphene Oxide (Fe₃O₄@GO) behaves as highly efficient and reusable heterogeneous nanocatalyst for alkene hydrogenation in the EtOH at 80 °C temperature using hydrazine hydrate as hydrogen source to deliver corresponding alkanes in good to excellent yields together with high TOF (>4500 h⁻¹) within 4-20 h reaction time.

Alkene hydrogenation catalyzed by expensive metal catalysts including Pd, Pt and Rh using hydrogen as reducing agent has emerged as an efficient protocol for petrochemical conversions and pharmaceuticals synthesis.¹ But the problems traditionally associated with these catalytic pathways are high cost of these precious metal catalysts, use of flammable hydrogen gas at high pressure and elevated temperatures. Considerable progress has been achieved with the first row transition-metal catalysts for catalytic alkene hydrogenation. Owing to high surface-to-volume ratio, transition-metal or metal oxide nanoparticles used as nanocatalysts nicely link the gap between ordinary homogeneous and heterogeneous metal based catalytic systems. Moores *et.al* have utilized polystyrene supported Fe(0) nanoparticles for alkene hydrogenation at 40 bar H₂ pressure.² New cobalt complexes have been designed by Chirik group for catalytic asymmetric alkene hydrogenation.³ Wangelin and co-workers have developed complex Co and Fe catalysts for hydrogenation of alkene at 1 bar H₂ pressure.⁴ Fe nanoparticles supported on functionalized graphene have been employed as catalyst by Breit group for catalytic alkene hydrogenation at 20 bar H₂ pressure requiring 24 h reaction time.⁵ Almost 100% conversion has been achieved for alkene hydrogenation at 10 bar H₂ pressure using Pd@Co/C catalyst.⁶ But all of these alkene hydrogenation catalysts involve use of H₂ at high pressure. So an alternative strategy for efficient alkene hydrogenation over a heterogeneous catalyst is highly desirable, which avoids highly flammable H₂ at high temperature.

Use of hydrazine hydrate as hydrogen source unlike H₂ (requiring high pressure) has gained a considerable importance as it facilitates easy handling and generation of only environmentally benign N₂ as a byproduct.⁷ Limitations regarding the hydrazine hydrate are storage and disposal in terms of atom economy. Upon contact with the strong oxidizing agents some exothermic reactions and evolution of gases may result and also this hydrogen source relies ultimately on ammonia synthesis which itself requires extreme high pressure of H₂. Alkene hydrogenation using hydrazine was carried out by different catalysts including guanidine,⁸ metal-organic framework⁹ and copper nanoparticles supported on diamond nanoparticles.¹⁰ Long reaction times and high catalyst loading (40 mol% catalyst loading) are major drawbacks.¹¹ Recently graphene and metal oxide nanoparticles are hugely recognized as reusable heterogeneous catalyst for conducting different types of organic transformations owing to their large surface area, high mechanical and hydrothermal stability.¹²

In this study, we have prepared magnetic Fe₃O₄ nanoparticles (5 nm and 15 nm) embedded on graphene oxide and carried out alkene hydrogenation over these magnetic Fe₃O₄@GO nanocatalyst using hydrazine hydrate as hydrogen



Scheme 1 Synthesis of Fe₃O₄@GO nanocatalyst and catalytic alkene hydrogenation reaction with this nanocatalyst using N₂H₄.H₂O as hydrogen source.

source. Magnetic separation of the catalyst, absence of flammable H_2 gas, high product selectivity, low catalyst loading and high recycling efficiency are the major advantages of $Fe_3O_4@GO$ nanocatalyst. As shown in Scheme 1, magnetically recoverable nanocatalysts $Fe_3O_4@GO$ bearing 5 and 15 nm Fe_3O_4 particle sizes have been synthesized by one step hydrothermal process using graphene oxide and anhydrous $FeCl_3$ at 200 °C for 4 and 10 h reaction time, respectively. Detailed experimental procedure for catalyst synthesis and comparison with existing, comparable materials is given in the ESI (S2). $Fe_3O_4@GO$ samples have been thoroughly characterized by wide angle powder XRD, TEM, XPS, Raman, FT-IR and AFM spectroscopic tools. The two nanocatalysts with the Fe_3O_4 sizes of 5 and 15 nm particle sizes are designated as $Fe_3O_4@GO-1$ and $Fe_3O_4@GO-2$, respectively.

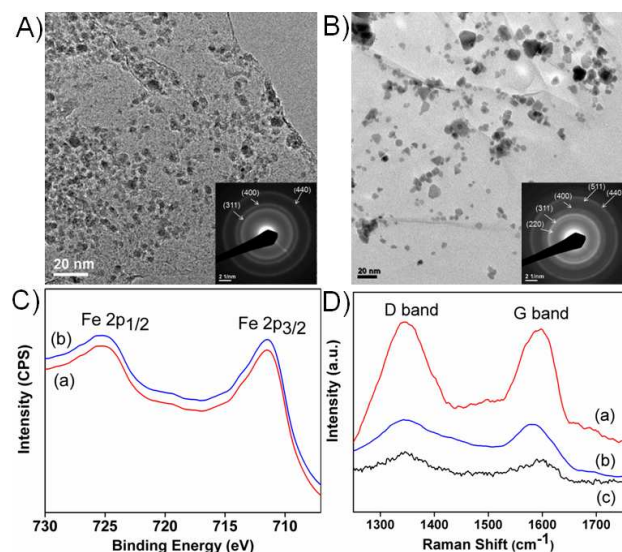


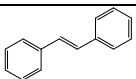
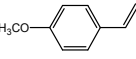
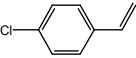
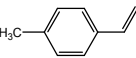
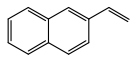
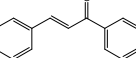
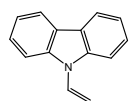
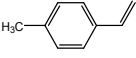
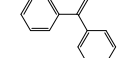
Fig. 1 (A and B) TEM images of $Fe_3O_4@GO-1$ and $Fe_3O_4@GO-2$ nanocatalysts, (C) High resolution XPS spectra and (D) Raman spectra of (a) $Fe_3O_4@GO-1$, (b) $Fe_3O_4@GO-2$ nanocatalysts and (c) GO respectively. Corresponding SAED patterns are given in the inset of (A) and (B).

TEM images (Fig. 1A and 1B) suggest that the Fe_3O_4 nanoparticles (black in color) with the size 5 nm and 15 nm are homogeneously dispersed throughout the graphene oxide surface of $Fe_3O_4@GO-1$ and $Fe_3O_4@GO-2$ nanocatalysts, respectively. Selected area electron diffraction (SAED) patterns (inset of Fig. 1A and 1B) confirm crystalline feature of Fe_3O_4 nanoparticles.¹³ In the X-ray photoelectron spectroscopy (XPS) spectra (Fig. 1C) the binding energy peaks centered at 711.5 eV and 725.2 eV, attributed to the $Fe2p_{3/2}$ and $Fe2p_{1/2}$ for Fe_3O_4 , respectively.¹⁴ The presence of graphene layer was confirmed by Raman spectroscopy which showed D band at 1348 cm^{-1} and G band at 1583 cm^{-1} (Fig. 1D).¹⁵ The I_D/I_G for $Fe_3O_4@GO-1$, $Fe_3O_4@GO-2$ and as synthesized GO are 1.06, 1.04 and 0.9, respectively, revealing molecular defects and reduction of GO in hydrothermal process. EDX pattern and elemental mapping (Figures S3 and S4, ESI) prove the presence of C, O and Fe elements in the $Fe_3O_4@GO$ materials. Wide angle powder XRD and FT-IR data are provided in Figures S5 and S8, ESI. AFM

topography images signify the cross sectional features of the $Fe_3O_4@GO$ nanocatalysts (Figure S10, ESI). The catalytic activity of $Fe_3O_4@GO$ nanocatalyst has been investigated in the alkene hydrogenation in EtOH solvent using hydrazine hydrate as reducing agent at 80°C (Scheme 1). All the products have been confirmed by GC-MS analysis. Detail catalytic procedure is provided in the section S2 of ESI. 4-chlorostyrene was chosen as model compound for this hydrogenation reaction (Table S1). With the gradual increase of $N_2H_4.H_2O$ (from 3.0 equivalents to 10.0 equivalents) catalytic reactions proceed faster (Table S1, entries 3-7). 10.0 equivalents $N_2H_4.H_2O$ is optimum to complete the reduction of without leaving any trace of incomplete reduction products (Table S1, entry 8). From the Table S1 it is quite evident that in EtOH at 80°C temperature is most suitable condition for hydrogenation reaction. $Fe_3O_4@GO-1$ nanocatalyst has been employed to achieve conversion 70% keeping other parameters same (Table S1, Entry 9). Under the same reaction conditions $Fe_3O_4@GO-2$ nanocatalyst resulted 99% conversion (Entry 8). This result indicates that large Fe_3O_4 nanoparticles (15 nm size) with high crystalline feature embedded on graphene oxide support are beneficial for the catalytic transfer hydrogenation reaction from hydrazine hydrate in EtOH medium. The Fe content in the $Fe_3O_4@GO-1$ and $Fe_3O_4@GO-2$ catalysts are 0.05298 $\mu mol/g$ and 0.1232 $\mu mol/g$, respectively determined by ICP-MS analysis, indicating that the reactions were carried out with 3.17×10^{-4} mol% and 7.39×10^{-4} mol% loading of iron. Catalytic reaction with bare Fe_3O_4 nanoparticles (Table S2, Entry 1) gives 45% conversion of 4-chlorostyrene, suggesting that graphene oxide has a promising role. Strong adsorption of organic molecules onto graphene oxide sheet is attributed to the π stacking and hydrophobic interactions that renders enhancement of catalytic conversion of $Fe_3O_4@GO$ nanocatalyst. Effect of catalyst dose on catalytic performance was evaluated by considering reaction with $Fe_3O_4@GO-2$ nanocatalyst with different mol% loading of Fe_3O_4 (Table S2).

Substrate scope was examined by carrying out alkene hydrogenation reaction with various alkenes over $Fe_3O_4@GO-2$. Electron donating styrenes (Table 1, entries 2 and 4) required long reaction times to yield corresponding substituted ethylbenzenes. 4-chlorostyrene and norbornene (Table 1, entries 3 and 7) showed 98-99% conversions in 4-6 h. Vinyl substituted polycyclic aromatic hydrocarbon (Table 1, entry 5) was reduced to corresponding ethyl derivative with 99% conversion at 18 h. Cyclic alkene cyclohexene underwent 86% conversion (Table 1, entry 6) but surprisingly very poor conversion was achieved for *cis*-cyclooctene (Table 1, entry 8) could be due to the presence of almost orthogonal allylic C-H bonds. Chemoselective reduction of C=C has been achieved for α,β -unsaturated ketone, chalcone (Table 1, entry 9) with 90% conversion. Successful hydrogenation was conducted for mono- and di-substituted alkenes (Table 1, entries 1 and 12). 9-vinylcarbazole (Table 1, entry 10) exhibited moderate conversion of alkene hydrogenation reaction. $Fe_3O_4@GO$ is also effective for the larger scale reaction with the consistent conversion (Table 1, entry 11). The TOF values range from

4650-33482 h⁻¹ and these are impressively high, suggesting

Entry	Alkene	Time (h)	Conversion ^b (%)	TOF×10 ² (h ⁻¹)
1		20	80	54.1
2		20	94	63.5
3		4	99	334.8
4		12	85	95.8
5		18	99	74.4
6		10	86	116.3
7		6	98	221
8		16	55	46.5
9		12	90	102
10		20	70	47.3
11 ^c		12	87	127.5
12		18	99	74.4

huge future potential of the Fe₃O₄@GO nanocatalyst.

Table 1 Hydrogenation of alkenes catalyzed by Fe₃O₄@GO-2^a

^aReaction conditions: Alkene (0.25 mmol), catalyst (15 mg), N₂H₄·H₂O (10 equivalent, 2.5 mmol, 125 mg), EtOH (3 mL), 80°C. ^b Determined by GC analysis. TOF= Turn over frequency (moles of substrate converted per mole of active sites per hour). All the products were confirmed by GC-MS analysis. ^cReaction was conducted with 10 mmol of 4-methylstyrene.

To confirm that the alkene hydrogenation catalytic reaction is indeed heterogeneous in nature, we have performed hot filtration test and leaching test by considering 4-methylstyrene as model substrate (See ESI, section S15). In order to check mechanical stability of Fe₃O₄@GO catalyst we have carried out TEM (Figure S13) and XPS (Figure S14A) analyses, which suggest that our catalyst is stable under reaction conditions. The efficacy of a Fe₃O₄@GO-2 nanocatalyst is also evident from its recyclability and stability (for example, no metal leaching). The catalyst can be efficiently recycled and reused for ten successive catalytic cycles for hydrogenation of 4-methylstyrene under optimized conditions (Figure S12, ESI). No leaching of Fe from Fe₃O₄@GO-2 catalyst is observed (AAS analysis, section S15, ESI), suggesting GO as an excellent support for the liquid phase catalytic reactions.¹⁶

In summary, Fe₃O₄ nanoparticles embedded on GO behaves as magnetically recoverable heterogeneous nanocatalyst for alkene hydrogenation with low catalyst loading using hydrazine hydrate as hydrogen source in EtOH at 80°C together with high

TOF of >4500 h⁻¹. This newly developed protocol avoids use of highly flammable H₂ gas at high pressure and temperature.

This work was financially supported by the Singapore National Research Foundation Fellowship (NRF2009NRF-RF001-015), the Singapore National Research Foundation CREATE program), Singapore Peking University Research Centre for a Sustainable Low-Carbon Future, and the NTU-A*Star Centre of Excellence for Silicon Technologies (A*Star SERC No.: 112 351 0003). AB thanks DST, New Delhi for financial support.

Notes and references

^a Division of Chemistry and Biological Chemistry, School of Physical and Mathematical Sciences, Nanyang Technological University, 21 Nanyang Link, Singapore 637371, Email: zhaoyanli@ntu.edu.sg.

^b Department of Materials Science, Indian Association for the Cultivation of Science, Jadavpur 700 032, India, Email: msab@iacs.res.in

^c School of Materials Science and Engineering, Nanyang Technological University, 50 Nanyang Avenue, Singapore 639798.

† Electronic Supplementary Information (ESI) available: synthesis, characterizations and catalysis details. See DOI: 10.1039/c000000x/

- J. G. de Vries and C. J. Elsevier, *Handbook of homogeneous hydrogenations*, Wiley-VCH, New York, 2007.
- R. Hudson, G. Hamasaka, T. Osako, Y. M. A. Yamada, C. -J. Li, Y. Uozumi and A. Moores, *Green Chem.*, 2013, **15**, 2141-2148.
- S. Monfette, Z. R. Turner, S. P. Semproni and P. J. Chirik, *J. Am. Chem. Soc.*, 2012, **134**, 4561-4564.
- D. Gartner, A. Welther, B. R. Rad, R. Wolf and A. Jacobi von Wangelin, *Angew. Chem. Int. Ed.*, 2014, **53**, 3722-3726.
- M. Stein, J. Wieland, P. Steurer, F. Tölle, R. Mulhaupt and B. Breit, *Adv. Synth. Catal.*, 2011, **353**, 523-527.
- Q. M. Kainz, R. Linhardt, R. N. Grass, G. Vilé, J. Pérez-Ramírez, W. J. Stark and O. Reiser, *Adv. Funct. Mater.*, 2014, **24**, 2020-2027.
- (a) E. W. Schmidt, *Hydrazine and Its Derivatives: Preparation, Properties, and Applications*, Wiley & Sons, New York, 2nd edn, 2001, vol. 1, p. 475; (b) W. M. N. Ratnayake, J. S. Grossert and R. Ackman, *J. Am. Oil Chem. Soc.*, 1990, **67**, 940; (c) R. K. Rai, A. Mahata, S. Mukhopadhyay, S. Gupta, P-Z. Li, K. T. Nguyen, Y. L. Zhao, B. Pathak and S. K. Singh, *Inorg. Chem.*, 2014, **53**, 2904-2909.
- M. Lamani, R. Siddappa, S. Guralamata and K. R. Prabhu, *Chem. Commun.*, 2012, **48**, 6583-6585.
- A. Dhakshinamoorthy, M. Alvaro and H. Garcia, *Adv. Synth. Catal.*, 2009, **351**, 2271-2276.
- A. Dhakshinamoorthy, S. Navalon, D. Sempere, M. Alvaro and H. Garcia, *Chem. Commun.*, 2013, **49**, 2359-2361.
- E. Kim, S. Kim and B. M. Kim, *Bull. Korean Chem. Soc.*, 2011, **32**, 3183-3186.
- (a) X. Huo, J. Liu, B. Wang, H. Zhang, Z. Yang, X. Sheb and P. Xia, *J. Mater. Chem. A*, 2013, **1**, 651-656; (b) T. Zeng, X. -L. Zhang, Y. -R. Ma, H. -Y. Niua and Y. -Q. Cai, *J. Mater. Chem.*, 2012, **22**, 18658-18663.
- J. Mondal, T. Sen and A. Bhaumik, *Dalton Trans.*, 2012, **41**, 6173-6181.
- Z-S. Wu, S. Yang, Y. Sun, K. Parvez, X. Feng and K. Mullen, *J. Am. Chem. Soc.*, 2012, **134**, 9082-9085.
- A. C. Ferrari and D. M. Basko, *Nat. Nanotechnol.*, 2013, **8**, 235-246.

- 16 J. Mondal, A. Modak, S. Basu, S. N. Jha, D. Bhattacharyya and A. Bhaumik, *Chem. Commun.* 2012, **48**, 8000-8002.